

<http://www.pjbs.org>

PJBS

ISSN 1028-8880

Pakistan Journal of Biological Sciences

ANSI*net*

Asian Network for Scientific Information
308 Lasani Town, Sargodha Road, Faisalabad - Pakistan

The Impact of Atmosphere Circular System on Coupling Features of Spring Net Primary Productivity with Precipitation in East Asia

¹Wu Gang, ^{1,4}Wang Yongxiang, ^{1,2}Yu Deyong, ²Pan Yaozhong, ^{1,4}Zhang Liang and ^{1,3}Shao Hongbo
¹State Key Laboratory of Urban and Regional Ecology, Research Center for Eco-Environmental Sciences,
Chinese Academy of Science, Beijing 100085, China
²College of Resources Science and Technology, Beijing Normal University,
Beijing 100875, China
³Institute of Life Sciences, Qingdao University of Science and Technology,
Qingdao 266042, China
⁴The Graduate School of Chinese Academy of Sciences, Beijing 100039, China

Abstract: In many East Asia regions, spring (from March to May) precipitation is an important restricting factor to vegetation growth. By analyzing the coupling features of spring NPP with precipitation, the result was found that the response features of NPP to precipitation were mainly embodied within the leading six NPP-precipitation paired-modes. The explanation rates of the leading six paired-modes to the covariance of NPP-precipitation were 42.91, 23.29, 9.96, 5.60, 5.04 and 3.95%, respectively and total to 90.75%. The temporal correlation coefficients of the leading six paired-modes were 0.830, 0.889, 0.841, 0.747, 0.912 and 0.923, respectively and all the correlations were significant at the level of 0.001. In some high altitude regions, there was no obviously corresponding relationship between NPP and precipitation in the leading two paired-modes and the reason of it may be that spring temperature was the main restricting factor to NPP. In middle and low altitude regions, the effect of precipitation on NPP was relatively more notable. Nine atmospheric circulation factors in spring affected the patterns of NPP and precipitation greatly and the affected regions with explanation rate to precipitation and NPP changes over 50% shared 65.58 and 60.41% to the whole study area, respectively.

Key words: Net primary productivity, precipitation, coupling feature, atmospheric circulation factor, remote sensing

INTRODUCTION

Essentially, Net Primary Productivity (NPP) is carbon-fixed by the terrestrial ecosystem and embodies its structure and function (Peng and Guo, 2000). In a thousand-year interval, climate change is the main reason of vegetation change and that non-climate factors are secondary (Whitlock and Bartlein, 1997). This shows that vegetation is sensitive to climate change. Solar radiation, temperature, precipitation, air humidity and carbon dioxide, which are the outside driving forces of the ecosystem, affect NPP by acting not only on vegetation directly, but also on the soil indirectly. The changes of vegetation precipitation demand, temperature and carbon dioxide content affect NPP most greatly. The effects of climate change on NPP are the comprehensive embodiment of the interaction of temperature, precipitation and carbon dioxide with vegetation and soil

(Chen, 1996; Willis *et al.*, 1997). The response of different ecosystems in different regions and seasons to the same climate conditions is obviously different. Precipitation affects NPP and its region distribution mainly by affecting water demand, water balance, carbon dioxide fixation of vegetation in the process of its photosynthesis. Water menace may result in leaf area attenuation (Kang, 1997), pore close (Tang, 1983) and transpiration and photosynthesis of vegetation may decline, which will reduce its dry matter accumulation. In general, properly increasing precipitation will prolong the growth period of vegetation, hence promoting NPP increase (Sala *et al.*, 1988). In dry regions, precipitation is the master restricting factor to NPP and NPP decreases with the ratio of precipitation quantity and potential evaporation quantity (Raich *et al.*, 1991; Melill *et al.*, 1993). Precipitation and its season distribution are directly correlative with NPP in grassland, hungriness and wetland (Sala *et al.*, 1988;

Corresponding Author: Dr. Yu Deyong, College of Resources Science and Technology, Beijing Normal University, Beijing 100875, China
Dr. Shao Hongbo, Institute of Life Sciences, Qingdao University of Science and Technology, Qingdao 266042, China

Stephenson, 1990). In some regions, there is a significant linear correlation between annually mean precipitation and above ground part of NPP (Sala *et al.*, 1988). For the crop, the effect of precipitation season change on its yield is more great (Whetton and Fowler, 1990). Water as the stuff of vegetation photosynthesis plays an important role in the process directly and on the other hand, it may affect NPP by adjusting the interaction process of the temperature, vegetation water demand and nutriment elements such as N and P etc (Melillo *et al.*, 1993).

Atmospheric circulation system, which affects larger regions and lasts for a long time, may control the change of climate system in some regions and some times by adjusting the distribution of precipitation and heat. In spring, water condition may be the restricting factor of vegetation growth in some regions, so playing an important role in NPP accumulation inevitably. In the Northern Hemisphere, people usually pay attention to some atmospheric circulation index such as ENSO (El Nino/South Oscillation), Arctic Oscillation (AO)/North Atlantic Oscillation (NAO), North Pacific (NP), Pacific/North American patterns (PNA), Eurasian (EU), West Atlantic (WA), West Pacific (WP), East Atlantic (EA). NAO is the most notable mode in the northern Atlantic regions. Although its most prominent scope is mainly in North America and Europe, climate system in some regions of Asia may accept its actions in spring (Dugam, 1997; Hurrell, 1995). AO is the most important and largest area scale mode for the North Hemisphere during wintertime (Tompson *et al.*, 2000) and is also notable until the coming spring (Tompson and Wallace, 1998; Tompson *et al.*, 2000).

In the past twenty years (1982-1999), climate and NPP changed remarkably and precipitation is an important factor impacting NPP in spring. The first aim of this study was to analyze the spatial response features of NPP in East Asia (70-170,10-70°N) to spring precipitation and the second task to discuss the role of atmospheric circulation factors in the response. All these will be helpful to understand the region differences of the response of the ecosystem to global changes.

MATERIALS AND METHODS

The remote sensing data used in this study were NOVA/AVHRR (Earth Resources Observation System, Pathfinder AVHRR Land Data Set) NDVI (Normalized Difference Vegetation Index) sets for East Asia (70-170,10-70°N) from 1982 to 1999, with 0.075°×0.075 spatial resolution and monthly temporal resolution. The land cover data were downloaded from Maryland University (ftp://hpssftp. umiacs. umd. edu/project/GLCF/Derived Data/ Global_Land_Cover/gl-latlong 8 km-landcover). The climate data included

monthly records of the precipitation, net radiation and average temperature and all had the same image spatial resolution and projection type as the NDVI data set.

Field measured NPP of different vegetation types came from the Oak Ridge National Laboratory Distributed Active Archive Center (NPP Database, http://www. daac. ornl. gov/NPP/npp_home.html) and National Forest Bureau of China. ENSO index came from Climate Prediction Center (USA). AO and NAO index were the observed value according to the definition by Thompson and Wallace (1998) and Hurrell (1995), respectively. NP index was the weighted mean air pressure of sea surface among 30-65°N and 160-140°W (Trenberth and Hurrell, 1994). According to the definition of Wallace and Gutzler (1981), other five atmospheric circulation indexes were calculated by the position height of 500 hPa in the troposphere.

The model of estimating NPP: CASA (Carnegie-Ames-Stanford Approach) NPP model can be described as:

$$NPP(x,t) = APAR(x,t) \times \epsilon(x,t) \quad (1)$$

$$\epsilon(x,t) = f_1(x,t) \cdot f_2(x,t) \cdot f_w(x,t) \cdot \epsilon_{max} \quad (2)$$

Where NPP(x,t) expresses net primary productivity of the vegetation in pixel x in time t. APAR(x,t) whose calculating method can be found in the reference (Potter *et al.*, 1993), Absorbed Photosynthetically Active Radiation (APAR) by the vegetation in pixel x and time t. $\epsilon(x,t)$ is the actual light utility efficiency. $f_1(x,t)$, $f_2(x,t)$ and $f_w(x,t)$ are the impact of temperature and water menace on the maximum light utility efficiency (ϵ_{max}) and its calculation method can be found in these references (Field 1995; Potter *et al.*, 1993; Zhang, 1990; Zhou and Zhang, 1995, 1996). Potter *et al.* (1993) and Field *et al.* (1995, 1998) set ϵ_{max} to 0.389 gC.MJ⁻¹ to drive CASA model and got 48.9 PgC (1 PgC = 10¹⁵ g Carbon) for global NPP. Jeffrey (2006) used two data sets of NCEP (National Centers for Environment Prediction) and GISS (Goddard Institute for Space Studies) to drive CASA model so as to compare the quality of the two data sets and he set the maximum light utility efficiency of different vegetation types in the two data sets as 0.46 g C.MJ⁻¹ and 0.50 gC.MJ⁻¹, respectively. Obviously, owing to the differences such as vegetation type, life conditions, ϵ_{max} for different vegetations should not be the same value. In this paper, we modeled ϵ_{max} for different vegetation types according to the principle of the minimum error between fielded NPP and modeled NPP. To some vegetation, the principle can be formulated as:

$$E(x) = \sum_i^j (m_i - n_i x)^2 x \in [\ell, u] \quad (3)$$

In formula (3), I and j express the sample number of the vegetation. m_i is fielded NPP and n is the product of APAR, temperature and water menace factors. x is the maximum light utility efficiency modeled for the vegetation. l and u are the lower and upper light utility efficiency of the vegetation, respectively. Formula (3) can be unwrapped as:

$$E(x) = \sum_{i=1}^j n_i^2 x^2 - 2 \sum_{i=1}^j m_i n_i x + \sum_{i=1}^j m_i^2 x \in [l, u] \quad (4)$$

Formula (4) is one degree and quadratic equation with an upward opening, so it has the minimum error from l to u . According to this principle, the values of ϵ_{\max} for different vegetation types in the study area are modeled as: Evergreen Needleleaf Forest 0.389 gC.MJ^{-1} , Evergreen Broadleaf Forest 0.978 gC.MJ^{-1} , Deciduous Needleleaf Forest 0.492 gC.MJ^{-1} , Deciduous Broadleaf Forest 0.664 gC.MJ^{-1} , Mixed Forest 0.490 gC.MJ^{-1} , Woodland 0.572 gC.MJ^{-1} , Wooded Grassland 0.557 gC.MJ^{-1} , Closed Shrubland 0.541 gC.MJ^{-1} , Open Shrubland 0.541 gC.MJ^{-1} , Grassland 0.541 gC.MJ^{-1} , Cropland 0.608 gC.MJ^{-1} , Bare Ground and Urban and build-up 0.541 gC.MJ^{-1} , Tundra 0.541 gC.MJ^{-1} .

The method of analyzing the spatial response features of NPP to spring precipitation: There are two element fields of X , which has P spatial points and Y , which has q spatial points. Each spatial point has n anomaly processed observed value. X and Y can be called the left field and the right field, respectively and can be described by the following matrices.

$$X = \begin{bmatrix} x_{11} & x_{12} & \dots & x_{1n} \\ x_{21} & x_{22} & \dots & x_{2n} \\ \vdots & \vdots & \dots & \vdots \\ x_{p1} & x_{p2} & \dots & x_{pn} \end{bmatrix} \quad Y = \begin{bmatrix} y_{11} & y_{12} & \dots & y_{1n} \\ y_{21} & y_{22} & \dots & y_{2n} \\ \vdots & \vdots & \dots & \vdots \\ y_{q1} & y_{q2} & \dots & y_{qn} \end{bmatrix} \quad (5)$$

$$SCF_k = \frac{\sigma_k^2}{\sum_{i=1}^m \sigma_i^2} \quad (6)$$

tokens the ratio of the covariance for the k -th paired-mode to the all between X and Y , so the lager of SCF_k , the more important is the k -th paired mode.

$$CSCF_N = \frac{\sum_{i=1}^N \sigma_i^2}{\sum_{i=1}^m \sigma_i^2} (N \leq m) \quad (7)$$

The above expressed the ratio of the covariance for the leading N paired modes to the all (m paired- modes)

between X and Y . The larger of $CSCF_N$, the more important are the leading N paired-modes and express the relationship of X , Y more accurately. This mathematical method can be called Singular Value Decomposition (SVD) and the details can be found in the reference (Wallace *et al.*, 1992). The paired-mode correlation coefficient was calculated by the corresponding temporal coefficient of the paired-mode between X and Y . The high correlation areas showed that the relationship between X and Y is very close. In this study, X and Y represented precipitation and NPP sequences, respectively.

Linear regress model of the nine atmospheric circular factors with NPP or precipitation: In some regions, NPP change may be impacted by multiple atmospheric circulation factors. At the same time, these factors may affect NPP pattern differently. It is necessary to differentiate the joint and individual impact on NPP of the nine atmospheric circulation factors.

To a pixel, there are normalized sequences Y_i (NPP) and $Z_{1i}, Z_{2i}, \dots, Z_{ni}$, which represent atmospheric circulation factors from 1 to n . The relationship of Y and Z can be formulated by multi-degree linear regress equation as:

$$\hat{y} = b_1 Z_{1i} + b_2 Z_{2i} + \dots + b_n Z_{ni} \quad (8)$$

In Eq. 8, I is the time length from 1982 to 1999 in this study and b_1, b_2, \dots and b_n are regression coefficients. It can be proved that:

$$C_2 = b_1 r_1 + b_2 r_2 + \dots + b_n r_n \quad (9)$$

Where c^2 is multi-correlation coefficient and r_1, r_2, \dots and r_n are the correlation coefficients of NPP with $Z_{1i}, Z_{2i}, \dots, Z_{ni}$, respectively. The left part of Eq. 9 is the joint contribution of the n atmospheric circulation factors to NPP deviation in the pixel and each item of the right part is the individual contribution of $Z_{1i}, Z_{2i}, \dots, Z_{ni}$, respectively.

RESULTS

The coupling features of spring NPP with precipitation: The results of SVD showed that the response features of NPP to precipitation in spring were mainly embodied in the leading six NPP-precipitation paired-modes. The first to the sixth paired-mode could explain 42.91, 23.29, 9.96, 5.60, 5.04 and 3.95% covariance of NPP-precipitation, respectively. The total explanation rate of the leading six paired-modes was 90.75%. Temporal correlation coefficients of the leading six paired-modes were 0.830, 0.889, 0.841, 0.747, 0.912 and 0.923, respectively and all the correlation was significant at the level of 0.001. So the

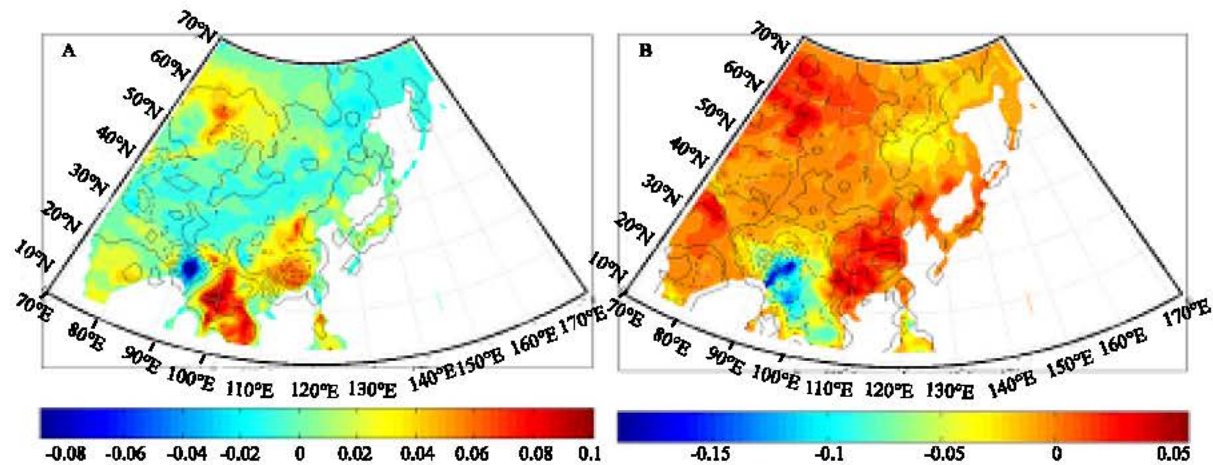


Fig. 1: The leading two paired-modes of spring NPP with precipitation by singular value decomposition. NPP shown in color. Precipitation shown in contours, with an interval of 0.03. Dashed lines indicated the negative values and solid lines indicated the positive values. Zero contours were omitted for simplicity and both units were arbitrary

Table 1: Correlation coefficients of the temporal coefficient of NPP-precipitation paired-modes with the nine atmosphere circumfluence factors in spring

Paired-mode	AO	EA	EU	NAO	NP	PNA	SO	WA	WP
NPP 1	0.21	0.17	0.39	0.07	0.18	-0.26	0.04	-0.11	-0.08
Precipitation 1	0.22	-0.16	0.21	0.19	0.37	-0.46	0.24	-0.17	-0.15
NPP2	0.13	0.01	0.08	0.47	0.07	-0.21	-0.31	0.07	-0.39
Precipitation 2	0.17	0.07	0.10	0.57 ^b	-0.05	-0.15	-0.46	0.00	-0.40
NPP 3	0.34	0.27	0.02	0.11	-0.25	0.30	-0.46	-0.03	-0.23
Precipitation 3	0.47 ^b	0.35	-0.03	0.23	-0.12	0.20	-0.55 ^b	-0.13	-0.22
NPP 4	-0.37	-0.15	-0.18	-0.22	-0.25	0.18	-0.24	0.18	-0.64 ^a
Precipitation 4	-0.46	-0.03	0.05	-0.35	-0.09	0.02	-0.08	0.17	-0.47 ^a
NPP 5	0.21	0.45	0.47 ^b	-0.05	0.27	-0.03	0.03	-0.13	0.39
Precipitation 5	0.03	0.54 ^b	0.30	-0.26	0.13	0.10	-0.05	-0.07	0.28
NPP 6	-0.17	-0.08	0.61 ^a	-0.15	0.11	-0.21	-0.14	-0.15	0.29
Precipitation 6	-0.16	-0.07	0.51 ^b	-0.17	-0.03	-0.14	-0.29	-0.17	0.13

^aThe correlation was significant at the level of 0.001; ^bthe correlation was significant at the level of 0.005

relationship of spring NPP with precipitation was very close and the most coupling features could be included in the leading six NPP-precipitation paired-modes. Spatial features of the first and the second paired-mode were illustrated as Fig. 1 A and B and the figures for the other four paired-modes were omitted here. The first and the second paired-mode with relatively larger geographical scale were more important, which was generally, the strongest NPP change center corresponding to the precipitation change center.

In the first paired-mode (Fig. 1A), the positive extreme value center of NPP mainly was located at the site in Thailand with altitude of 20°N and longitude of 100°E and corresponded to the positive center of precipitation. The coupling negative extreme value center of NPP with precipitation was located at the site in Bengal with altitude of 25°N and longitude of 92°E. Change trend between NPP and precipitation near the areas of the two coupling center was synchronous. At the site with altitude of 57°N and longitude of 85°E in Guangdong province of China, change trend of positive NPP center and negative precipitation center was contrary.

In the second paired-mode (Fig. 1B), negative coupling NPP-precipitation extreme value center at the site with altitude of 25°N and longitude of 93°E in Bengal changed synchronously. In addition, in some areas of east China and parts of middle Japan, positive NPP and precipitation coupling centers changed synchronously.

In the whole, coupling features of NPP-precipitation in the areas of low altitude were more obvious than in the high altitude areas (Fig. 1). The main reason may be that temperature and heat conditions were the key restricting factors to vegetation growth in the high altitude areas, but precipitation impacted vegetation growth more greatly in the low altitude areas.

Correlation analysis of NPP-precipitation paired-modes with atmospheric circulation factors: In this study, we mainly considered the impact of the nine atmospheric circulation factors (SO, NAO, EU, WP, EA, PNA and NP) on NPP-precipitation coupling features. Correlation coefficients of NPP-precipitation paired-modes by singular value decomposition with the nine atmosphere circulation factors were listed as Table 1.

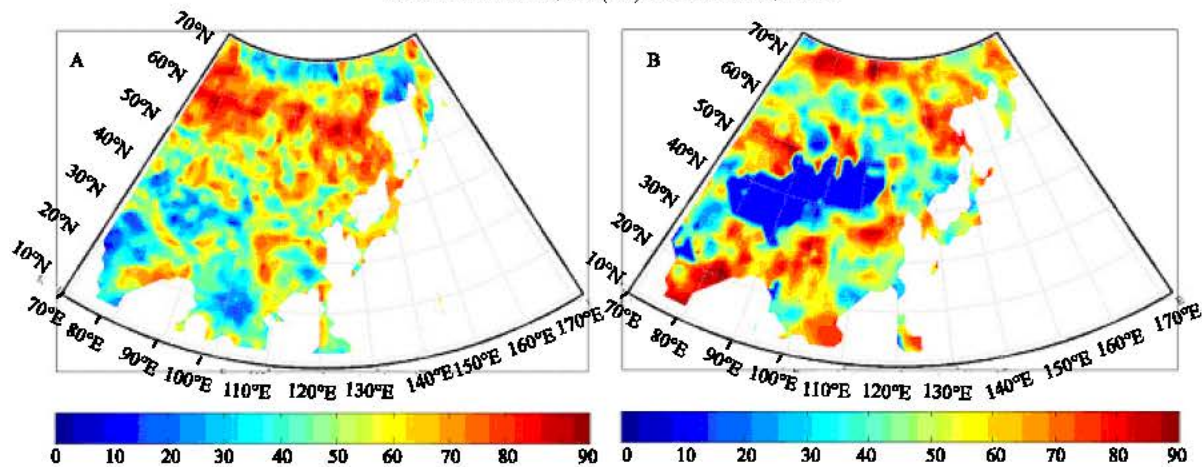


Fig. 2: The explanation rates of atmosphere circumfluence factors to spring NPP deviation (A) and spring precipitation deviation (B)

Table 2: Correlation coefficients of atmosphere circumfluence factors with each other in spring

Factors	AO	EA	EU	NAO	NP	PNA	SO	WA	WP
AO	1.00	-0.01	-0.11	0.77 ^a	0.51 ^b	-0.30	-0.01	-0.56 ^b	0.15
EA		1.00	0.13	-0.24	-0.03	0.08	-0.39	0.16	-0.12
EU			1.00	-0.11	-0.05	0.07	-0.17	0.07	0.30
NAO				1.00	0.24	-0.16	-0.20	-0.34	0.01
NP					1.00 ^a	-0.83 ^a	0.53 ^b	-0.56 ^b	0.14
PNA						1.00	-0.48 ^b	0.43	0.14
SO							1.00	-0.06	0.37
WA								1.00	-0.17
WP									1.00

^aThe correlation relationship was significant at the level of 0.001; ^bthe correlation relationship was significant at the level of 0.005

There was no significant correlation in the first NPP-precipitation paired-mode, but the impact of AO, EU, NP and PNA was relatively important. The relationship of the second precipitation mode with NAP was closer and correlation coefficient was 0.57. Correlation coefficients of the second precipitation with AO and SO were 0.47 and 0.55, respectively. Correlation coefficients of the fourth, fifth and sixth precipitation mode with WP, EA and EU were -0.47, 0.54 and 0.51, respectively. All the above correlation was significant at the level of 0.005. Correlation coefficients of the fourth and sixth NPP mode with WP and EU were -0.64 and 0.61, respectively and the correlation was significant at the level of 0.001. Correlation coefficients of the fifth NPP mode with EU were 0.47 and the correlation was significant at the level of 0.005. So it could be concluded that AO, EA, EU, NAO, SO and WP impacted spring NPP and precipitation obviously. Especially, the impacts of EU on the sixth NPP-precipitation paired-mode and WP on the fourth NPP-precipitation paired-mode was very great. When the signal of EU was strong, it was favorable to NPP and precipitation addition, but WP was contrary to this trend.

Individual atmospheric circulation factor had different impacts on different regions. Some regions may be

impacted by many factors and these factors usually tended to be dependent and jointly acted on climate system and vegetation activity. There were significant correlations Of NAO, NP, WA with AO, of NP with PNA and of SO, WA, SO with PNA (Table 2).

Regress analysis of NPP with atmospheric circulation factors: Observed NPP and the nine atmospheric circulation indexes were normalized firstly. To a pixel, regression equation could be built with NPP as the dependent variable and the nine factors as the independent variables. According to the regression equation and the nine factors, calculated NPP value could be gotten. The ratio of calculated NPP deviation with observed NPP deviation reflected the joint impact of the nine factors on NPP change. The right part of formula (9) could differentiate the separate impact of the individual circulation factor on NPP change.

Explanation rate of individual atmospheric circulation factor to NPP deviation was listed in Table 3 (spatial impact map of individual factor to NPP omitted here) and spatial distribution of the joint impact of the nine atmospheric circulation factors on NPP deviation was show as Fig. 2A. The areas with high explanation rate of

Table 3: Area percentage of the regions impacted by the individual atmospheric circulation factor (%)

Factors	Explanation rate <30%	30%≤Explanation rate <50%	Explanation rate ≥50%
AO	87.60	8.22	4.18
EA	88.09	10.33	1.58
EU	84.81	11.31	3.88
NAO	93.78	5.40	0.82
NP	96.14	3.36	0.50
PNA	93.16	4.93	1.91
SO	89.19	8.34	2.47
WA	86.55	12.84	0.61
WP	83.45	13.56	2.99

Note: The area percentage in this table meant the ratio of the region with some explanation rate to the whole region impacted by the atmospheric circulation factor

AO to NPP deviation were mainly located in northeast and Xinjiang municipality of China. The areas with high explanation rate of EA to NPP deviation were mainly located near the north part of 40°N such as Xinjiang municipality, Gansu province and Inner Mongolia of China and some regions with altitude from 50°N to 66°N and longitude from 100 to 140°E in Russia. The impact core of NP to NPP deviation was centered in the regions within 50-70°N and 70-90°E. NAO mainly impacted the north part of Kamchatka Peninsula in Russia. The impact of NP on the study area was relatively weak in spring and mainly focused within the scope of 20-40°N. PNA mainly affected the north part adjacent to 140°E and the impact core of SO to NPP deviation centered at the areas near the point with altitude of 57°N and longitude of 120°E. The high explanation rate of WA to NPP deviation was mainly located in the regions near the point with altitude of 50°N and longitude of 123°E and WP mainly impacted the areas near the sea and with altitude scope from 20 to 50°N and longitude scope from 110 to 140°E.

The regions with the highest explanation rate of the nine atmospheric circulation factors to spring NPP deviation were mainly located within the altitude from 50 to 65°N, especially the areas near the 60°N altitude line (Fig. 2A). Percentages of the regions with explanation rate over 80%, between 50 and 80% and lower than 50% were 10.46, 55.12 and 34.2%, respectively. The percentage of the regions with explanation rate over 50% totaled to 65.58%, so the nine atmospheric circulation factors impacted NPP in spring greatly.

Vegetation growth process was controlled directly by many factors such as precipitation and temperature. Usually, when atmospheric circulation system changes, some local climate factors such as precipitation also changes subsequently, because of which atmospheric circulation system plays an indirect impact on vegetation growth. How does atmospheric circulation system affect the tem-spatial pattern of precipitation? We also used the same regression methods to choose precipitation of the pixel as the dependent variable and the nine atmospheric circulation factors as the independent variables and built a multiple linear regression equation. Spatial explanation rate of the nine atmospheric circulation factors to spring precipitation pattern was shown as Fig. 2B.

The percentages of the regions with explanation rate over 80%, between 50 and 80% and lower than 50% were 7.44, 52.9 and 39.5%, respectively. The nine atmospheric circulation factors explained 60.41% precipitation change of the areas with explanation rate over 50%, so these factors impacted spring precipitation pattern greatly. Dissert and hungriness near the boundary of west northern China, Mongolia and Kazakstan (the dark blue areas in Fig. 2B) with little precipitation in spring were weakly influenced by the nine atmospheric circulation factors.

DISCUSSION

In order to quantitatively analyze, we chose three regions with distinct coupling features of NPP with precipitation to build the regression equation between NPP and the nine atmospheric circulation factors and compared the change trend of observed and calculated NPP. The three regions included Bengal (22-25°N, 90-93°E), south China (25-30°N, 110-115°E), and Thailand (16-25°N, 97-102°E) and the variation trend of mean NPP for the three selected region was shown as Fig. 3.

Obviously, observed NPP significantly correlated with calculated NPP by the nine atmospheric circulation factors in the three selected regions (Fig. 3). All the correlations were significant at the level of 0.001. Bengal and Thailand had the lowest and highest correlation coefficients of 0.692 and 0.762, respectively. So observed NPP of the three selected regions were very close with the nine atmospheric circulation factors more easily in spring. NPP of the three regions all tended to increase from 1982 to 1999. South of China (25-30°N, 110-115°E) with annual mean 2.9187 gC m⁻² increasing had the most notable increase trend and was the advanced agriculture zone of China. Explanation rate of the nine atmospheric circulation factors to NPP deviation in Bengal (22-25°N, 90-93°E), south China (25-30°N, 110-115°E) and Thailand (16-25°N, 97-102°E) were 54.09, 49.34 and 51.14%, respectively.

Figure 4 (A) and (C) showed that NPP was significantly correlated with precipitation at the level of 0.001 and 0.005, respectively. Negative correlation showed that Fig. 4B was not significant. It could be supposed

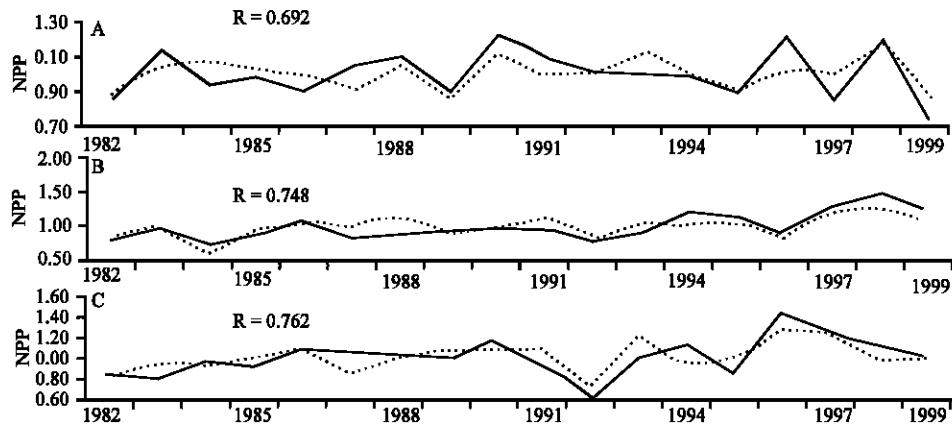


Fig. 3: Variation change of NPP for the three selected regions in spring. NPP was in anomaly format with respect to 1982-1999. Shown in solid lines were the trend of observed value and the dashed lines were the trend of regression value by atmosphere circulation factors. (A) Bengal, (B) south China, (C) Thailand

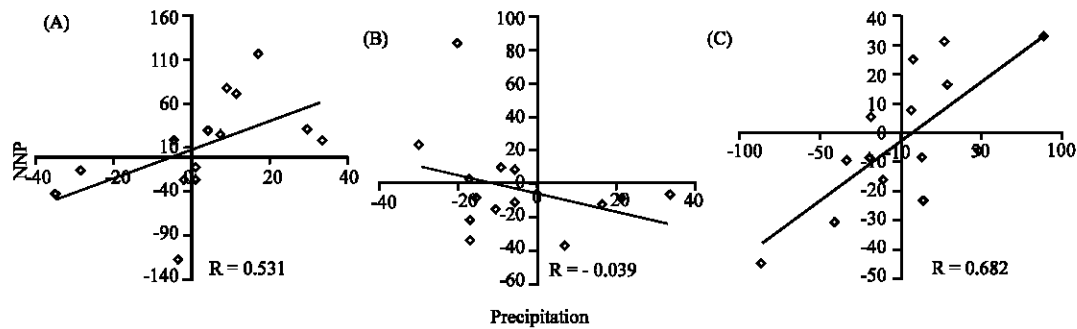


Fig. 4: Scattered plots of mean NPP and precipitation for the three selected regions from 1982 to 1999. NPP and precipitation were observed anomaly value with respect to 1982-1999. (A) Bengal (22-25°N,90-93°E), (B) south China (25-30°N,110-115°E), (C) Thailand(16-25°N,97-102°E)

that the significant correlation of NPP with atmospheric circulation system in the selected regions should be connected by precipitation. What extent do these atmospheric circulation factors impact the precipitation pattern? We also used the regression analysis methods and chose precipitation as the dependent variable and the nine atmospheric circulation factors as the independent variable to build regression equation. Mean contribution rates of the nine atmospheric circulation factors to precipitation pattern in Bengal (22-25°N,90-93°E), south China (25-30°N,110-115°E) and Thailand (16-25°N, 97-102°E) were 49.77, 43.74, 36.25%, respectively. The results showed that coupling features of NPP with precipitation in the selected regions were intensively impacted by the nine atmospheric circulation factors.

According to Fig. 2, explanation rate of the nine atmospheric circulation factors to spring NPP was higher than spring precipitation in the longitude scope from 50 to 65°N. Coupling features of the leading paired-modes of

NPP-precipitation in the longitude scope were also not notable. Obviously, precipitation only was one of the factors that caused NPP variation, but not the key and sole factor.

In the whole, the nine atmospheric circulation factors influenced coupling features of spring NPP and precipitation more greatly in the areas south to 30°N altitude line. Although spring NPP and precipitation were impacted by the nine atmospheric circulation factors greatly in many regions, some change trends were still not explained completely. The possible reasons may be that: 1) local micro climate and other environment conditions were not considered; 2) NPP change in the middle and high altitude areas may be more sensitive to temperature than to precipitation; 3) In some regions, the relationship of NPP and precipitation with the nine atmospheric circulation factors was not simply linear, so the multi-factor linear model was not suitable to study the relationship among them and 4) Besides the nine

atmospheric circulation factors, other larger scale of climate system such as East Asia monsoon may influence spring NPP and precipitation pattern in spring. All these uncertain possibilities must be discussed in the future study.

CONCLUSIONS

Spatial response features of spring NPP to precipitation are mainly included in the six leading paired-modes, which explains 90.75% of their covariance. All correlations of the leading six temporal coefficients of NPP and precipitation are significant at the level of 0.001. So the relationship of spring NPP with precipitation is very close and the most notable coupling features come out in the negative coupling core of Bengal (22-25°N, 90-93°E) and positive coupling core of Thailand (16-25°N, 97-102°E) in the first NPP-precipitation paired-mode by singular value decomposition.

Atmospheric circulation system plays a great role in coupling features of spring NPP with precipitation and usually, they tend to jointly influence them. The percentages of the regions with explanation rate of the nine atmospheric circulation factors to spring NPP and precipitation pattern over 50% total to 65.58 and 60.41%, respectively. So spring NPP and precipitation are greatly influenced by these circulation factors.

Atmospheric circulation system is the original driving force for spring precipitation pattern. Some researches have showed that atmospheric circulation system also changed in a long span of time and caused different response of vegetation in different regions to global change. Vegetation in the regions more easily influenced by it will be more sensitive to climate change.

ACKNOWLEDGMENTS

This research was funded by the National Natural Science Foundation of China (Grant No. 40473054, 40371001) and Achievement Transformation Foundation of Agricultural Science and Technology (05EFN216600446') and Specialized Initiation Foundation of Excellent Ph.D Thesis of Chinese Academy of Sciences. Thanks are also given to references and editors whose comments improved the quality of the manuscript.

REFERENCES

Chen, D.X., H.W. Hunt and J.A. Morgan, 1996. Responses of a C₃ and C₄ perennial grass to CO₂ enrichment and climate change: Comparison between model predictions and experimental data. *Ecol. Modeling*, 87: 11-27.

Dugam, S.S., S.B. Kakade and R.K. Verma, 1997. Interannual and long-term variability in the north atlantic oscillation and indian summer monsoon rainfall. *Theor. Applied Climatol.*, 58: 21-29.

Epstein, H.E., W.K. Lauenroth and I.C. Burke, 1997. Productivity patterns of C₃ and C₄ functional types in the U.S Great Plains. *Ecology*, 78: 722-731.

Field, C.B., J.T. Randerson and C.M. Maimstrom, 1995. Global net primary production: Combining ecology and remote sensing. *Remote Sen. Environ.*, 51: 74-88.

Field, C.B., M.J. Behrenfeld and J.T. Randerson, 1998. Primary production of the bio sphere: Integrating terrestrial and oceanic components. *Science*, 281: 237-240.

Hurrell, J.W., 1995. Decadal trends in the North Atlantic Oscillation: Regional temperatures and precipitation. *Science*, 269: 676-679.

Jeffrey, A.H., 2006. NCEP and GISS solar radiation data sets available for ecosystem modeling: Description, differences and impacts on net primary production. *Global Biogeochem. Cycles*, 19: 1-18.

Kang, S.Z., H.J. Cai and Y.L. Liang, 1997. On the study of the effects of elevated CO₂ concentration on the canopy temperature, evapotranspiration and soil water condition of sp. ring wheat. *Acta Ecol. Sin.*, 17: 412-417.

Melillo, J.M., D.W. Kicklighter and A.D. McGuire, 1993. Global climate change and terrestrial net primary production. *Nature*, 363: 234-240.

Peng, S.L. and Z.H. Guo, 2000. Use of GIS and RS to estimate the light utilization efficiency of the vegetation in Guangdong, China. *Acta Ecologica Sin.*, 20: 903-909.

Potter, C.S., J.T. Randerson and C.B. Field, 1993. Terrestrial ecosystem production: A process model based on global satellite and surface data. *Global Biogeochem. Cycles*, 7: 811-841.

Raich, J.W., E.B. Rastetter and J.M. Melillo, 1991. Potential net primary production in South America: Application of a global model. *Ecol. Appl.*, 1: 399-429.

Sala, O.E., M.E. Biondini and W.K. Lauenroth, 1988. Primary production of the central grasslands region of the United States. *Ecology*, 69: 40-45.

Stephenson, N.L., 1990. Climatic control of vegetation distribution: The role of the water balance. *Am. Natur.*, 135: 649-670.

Tang, Z.C., 1983. On the study of drought ecophysiology in plants. *Acta Ecol. Sin.*, 3: 196-203.

Tompson, D.W.J. and J.M. Wallace, 1998. The Arctic Oscillation signature in the wintertime geopotential height and temperature fields. *Geophys. Res. Lett.*, 25: 1297-1300.

- Tompson, D.W.J., J.M. Wallace and G.C. Hegerl, 2000. Annular modes in the extratropical circulation, PartII: Trends J. Climate, 13: 1018-1036.
- Trenberth, K.E. and J.W. Hurrell, 1994. Decadal atmosphere-ocean variations in the Pacific. Climate Dynamics, 9: 303-319.
- Wallace, J.M. and D.S. Gutzler, 1981. Teleconnections in the geopotential height field during the Northern Hemisphere winter. Monthly Weather Revi., 109: 784-812.
- Wallace, J.M., C. Smith and C.S. Bretherton, 1992. Singular value decomposition of Wintertime sea surface temperature and 500 mb height anomalies. J. Climate, 5: 561-576
- Whetton, P.H. and A.M. Fowler, 1993. Haylock M.R. Implications of climate change due to enhanced greenhouse effect on floods and droughts in Australia and New Zealand. Climatic Change, 25: 289-317.
- Whitlock, C. and P.J. Bartlein, 1997. Vegetation and climate change in northwest America during the past 125kyr. Nature, 388: 57-60.
- Willis, K.J., M. Braun and P. Sumegi, 1997. Does soil change cause vegetation change or vice versa? A temporal perspective from Hungary. Ecology, 78: 740-750.
- Zhang, Z.M., 1990. The rule and method of calculating evaporation. University of Science and Technology Chengdu Press. Chengdu, China, pp: 216-223.
- Zhou, G.S. and X.S. Zhang, 1995. A natural vegetation NPP model. Acta Phytoecol. Sin., 19: 193-200.
- Zhou, G.S. and X.S. Zhang, 1996. Study on climate-vegetation classification for global change in China, Acta Phytoecol. Sin., 38: 8-17.